

UC Irvine

UC Irvine Previously Published Works

Title

Sensitivity analysis of a Vision 21 coal based zero emission power plant

Permalink

<https://escholarship.org/uc/item/3q17t9tn>

Journal

Journal of Power Sources, 158(1)

ISSN

0378-7753

Authors

Verma, A

Rao, AD

Samuelsen, GS

Publication Date

2006-07-01

DOI

10.1016/j.jpowsour.2005.09.015

Copyright Information

This work is made available under the terms of a Creative Commons Attribution License, available at

<https://creativecommons.org/licenses/by/4.0/>

Peer reviewed

Sensitivity analysis of a Vision 21 coal based zero emission power plant

A. Verma, A.D. Rao, G.S. Samuelsen*

Advanced Power Energy Program, University of California, Irvine, CA 92697-3550, USA

Received 14 August 2005; accepted 9 September 2005

Available online 14 February 2006

Abstract

The goal of the U.S. Department of Energy's (DOE's) FutureGen project initiative is to develop and demonstrate technology for ultra clean 21st century energy plants that effectively remove environmental concerns associated with the use of fossil fuels for producing electricity, and simultaneously develop highly efficient and cost-effective power plants. The design optimization of an advanced FutureGen plant consisting of an advanced transport reactor (ATR) for coal gasification to generate syngas to fuel an integrated solid oxide fuel cell (SOFC) combined cycle is presented. The overall plant analysis of a baseline system design is performed by identifying the major factors effecting plant performance; these major factors being identified by a strategy consisting of the application of design of experiments (DOEx). A steady state simulation tool is used to perform sensitivity analysis to verify the factors identified through DOEx, and then to perform parametric analysis to identify optimum values for maximum system efficiency. Modifications to baseline system design are made to attain higher system efficiency and to lower the negative impact of reducing the SOFC operating pressure on system efficiency.

© 2006 Published by Elsevier B.V.

Keywords: Solid oxide fuel cell (SOFC); Design of experiments (DOEx); Integrated coal gasification fuel cell combined cycle (IGFC); Zero emission; SOFC hybrid

1. Introduction

Under the sponsorship of the U.S. Department of Energy (DOE)/National Energy Technology Laboratory (N.E.T.L), the Advanced Power and Energy Program (APEP) of the University of California, Irvine, is defining the system engineering issues associated with the integration of key components and subsystems into power plant systems that meet performance and emission goals of the FutureGen program [1,2]. The design analysis of an advanced FutureGen plant that consists of coal gasification to generate a clean syngas to fuel a solid oxide fuel cell (SOFC)/gas turbine combined cycle hybrid is presented.

The overall plant analysis of a baseline system design is performed by identifying the major factors effecting plant performance using DOEx. DOEx also assists in identifying higher order interactions which cannot be pointed out using parametric analysis. The advanced power systems analysis tool (APSAT), a steady state simulation tool developed by APEP for the analyses of advanced power and energy plants, [3,4] is used to perform the sensitivity analysis, to verify the factors identi-

fied through DOEx, and then to perform parametric analysis to identify design point operating parameters for maximum system efficiency.

In particular, modifications to baseline system design are made in order to achieve higher system efficiency while lowering the negative impact of reducing the SOFC operating pressure on system efficiency. Although Siemens Westinghouse (then Westinghouse) had successfully tested a tubular SOFC at a pressure of 1520 kPa under a DOE contract (DE-FC21-91MC28055), lower SOFC operating pressures are very desirable since there are challenges associated with developing the required seals as well as the materials for fuel cells operating at high pressures (HP). The dynamic behavior of the hybrid during plant trips is also a concern at high fuel cell operating pressures.

1.1. Design inputs

The design ambient conditions consist of utilizing ISO ambient conditions of 15 °C (59 °F) dry bulb temperature, 60% relative humidity and sea level. Mechanical draft cooling towers are utilized for plant heat rejection with a 3.9 °C (7 °F) approach to the wet bulb temperature. A temperature rise of 11.1 °C (20 °F) is assumed for the cooling water while a 5.6 °C (10 °F) approach temperature is utilized in the steam turbine surface condenser.

* Corresponding author. Tel.: +1 949 824 5468; fax: +1 949 824 7423.
E-mail address: gss@nrcr.uci.edu (G.S. Samuelsen).

Table 1
Analysis of Illinois no. 6 coal

Proximate analysis (wt.%)	
Fixed carbon	47.05
Volatile matter	30.91
Moisture content	11.12
Ash content	10.91
Ultimate analysis (wt.%)	
Ash	10.91
C	71.72
H	5.06
O	7.75
N	1.41
S	2.82
Cl	0.33
Total	100
Heating values (MJ kg ⁻¹)	
Higher heating value	27139.90
Lower heating value	26139.21

Table 2
Key equipment design basis

Equipment	Design point
Gasifier	
Operating pressure (kPa)	3048
Raw syngas exit temperature (°C)	1052
Syngas expander	
Expander isentropic efficiency (%)	88.0
Generator efficiency (%)	98.0
SOFC	
Operating pressure (kPa)	1880
Operating temperature (°C)	800
Fuel utilization (%)	85
Voltage (V)	0.75
Inverter efficiency (%)	97
Excess air (%)	100
ITM operating temperature (°C)	800
Gas turbine	
Compressor isentropic efficiency (%)	90
Expander isentropic efficiency (%)	93
Generator efficiency (%)	98.6
Steam turbine	
HP isentropic efficiency (%)	83.6
IP isentropic efficiency (%)	90.7
LP isentropic efficiency (%)	84.3
Generator efficiency (%)	98.0

The feedstock consists of Illinois no. 6 coal, which has the composition shown in Table 1.

The design basis for the key equipment for the baseline plant design is summarized in Table 2.

2. Baseline coal based zero emission power plant description

As depicted in Fig. 1, the major features of this configuration include an O₂ blown ATR, the O₂ being supplied by an ion or O₂ transport membrane (ITM/OTM) unit [5,6], separate SOFC anode and cathode exhaust streams, and a shift conversion unit

followed by a high temperature H₂ separation membrane, to separate hydrogen and recycle it back to the SOFC anode fuel stream in order to capture the gaseous carbon emissions from the gasifier (95% of the total carbon fed to the gasifier) as CO₂ for sequestration. Ground Coal along with ground limestone (both <500 μm particle size) for in-bed sulfur capture (about 85% of the sulfur is expected to be captured along with over 90% of the chlorine) is added to the upper stage of the mixing zone. The gas exits the top of the gasifier riser and goes to a primary cyclone that is connected to a standpipe that receives the unreacted char and ash/bed material for recirculation back to the mixing zone. The overall carbon conversion for this O₂ blown ATR is assumed to be 95% based on information provided by Southern Services Company who operates the Wilsonville process demonstration unit [7].

Ash withdrawn from the ATR has very little carbon in it and its mass median diameter (MMD) is about 150 μm (coarse ash) and has the appearance of beach sand. It could be utilized as bed material for a fluidized bed unit. The gas leaving the ATR enters a particulate control device (PCD). The ash withdrawn from the PCD has an MMD of about 15 μm (fine ash or char) and typically has 30% carbon and a BTU value of about 5500 Btu lb⁻¹. This fine ash or char is in powdery form and is not in a vitrified state. More than 95% of CaS is present in the fine ash. Based on data collected at the Wilsonville process demonstration unit, the reactive CaS content of the fine ash should not exceed 500 ppm (when the reactive CaS exceeds 500 ppm, the ash is considered as hazardous). The syngas leaves the gasifier at approximately 1050 °C based again on information provided by Southern Services Company. The syngas is cooled to 400 °C by generating superheated steam. It then goes to a barrier filter where over 99.99% of the remaining particulates are removed.

Next the syngas is fed to a chloride guard bed containing nahcolite, which also removes any other remaining halides. From the chloride guard which is followed by another barrier filter, the fuel gas goes to a zinc titanate bed for sulfur removal, and then to final particulate filters. A fraction of the syngas is utilized as transport gas for feeding the solids to the ATR. The required amount of gas is first cooled in a series of heat exchangers while providing heat for high pressure steam generation and for the humidifier. The syngas is next further cooled against cooling water, and then compressed to the required pressure. A closed loop CO₂ system provides the gas required for pressurization of the lock hoppers, while the required make-up CO₂ is supplied from the captured CO₂ [7].

The remainder of the clean syngas is passed through a fixed bed reactor containing the Amended SilicatesTM sorbent where the mercury is chemisorbed. The clean syngas is combined with steam, and then fed to a fixed bed reactor containing a methanation catalyst followed by a turbo-expander [8]. The methanation/shift reactions that occur within the reactor serve to (1) producing additional methane (in addition to that generated within the ATR) and (2) raising the temperature of the syngas (from 372 to 716 °C). The increased methane content of the syngas assists in providing a heat sink (by the endothermic reforming reaction) for the heat generated within the SOFC while the increased temperature of the syngas increases the

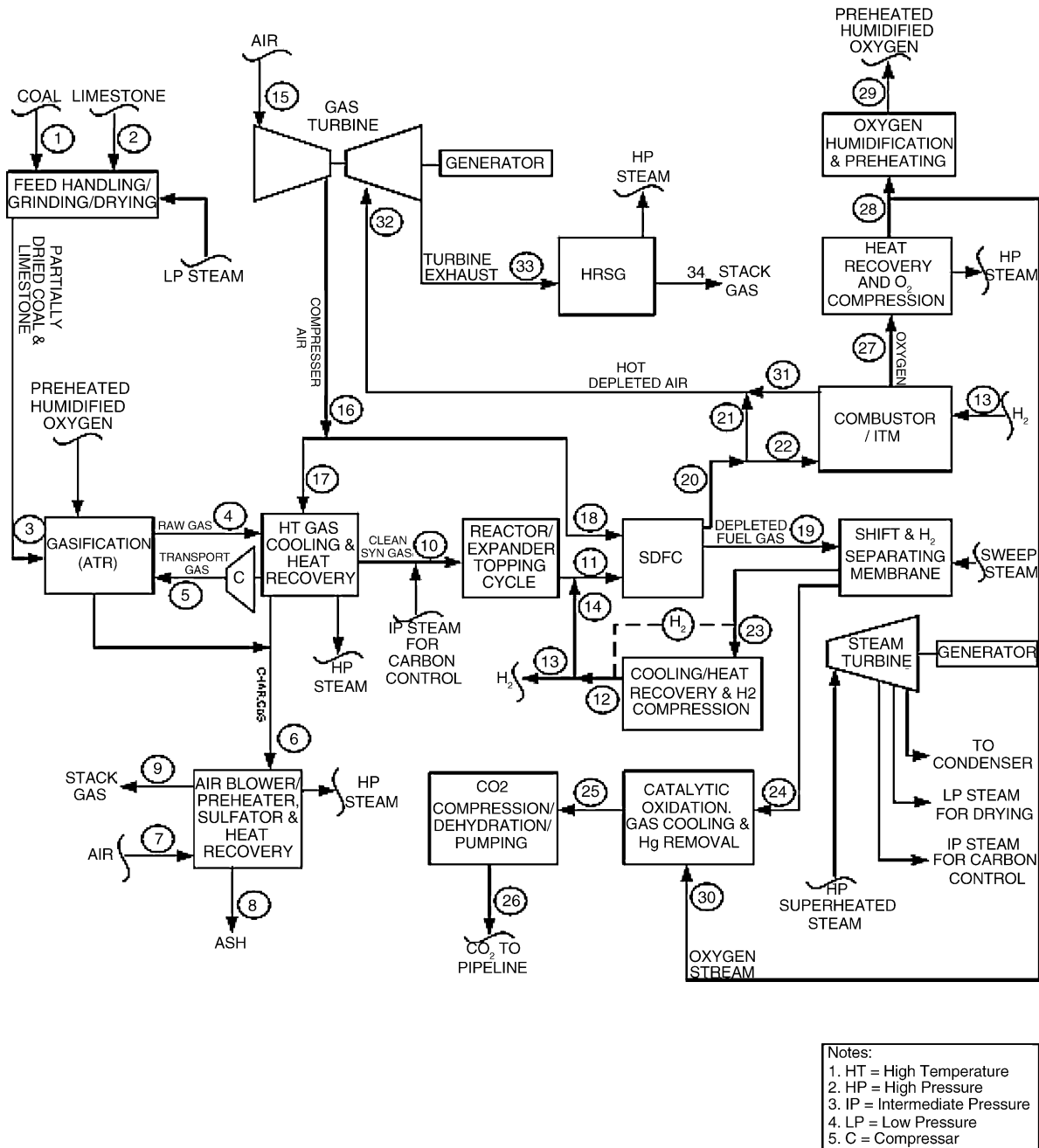


Fig. 1. Block sketch of baseline Vision 21 coal based zero emission power plant.

power developed by the turbo-expander which expands the syngas from a pressure of 2310 to 1880 kPa. It also reduces the amount of heat exchange required within the SOFC system. Steam is added to the syngas upstream of the shift/membrane unit to avoid carbon deposition within that unit as well as in the downstream methanation reactor and in the reformer located within the SOFC stack [7].

A chloride guard bed consisting of Na on alumina followed by a sulfur guard bed consisting of alternating layers of COS hydrolysis catalyst, such as a Co-Mo or a Ni-Mo catalyst and ZnO for the H₂S capture (purple sandwich) may be included upstream of the methanator as a final cleanup step to remove any trace amounts of the chlorides and sulfur compounds to the level

required by the methanation catalyst (and the reforming catalyst within the SOFC system) of 0.1 ppmV for each of these impurities. The methanated/expanded syngas after being preheated and reformed within the SOFC module is fed to the anode side of the cells. Compressed air supplied by the gas turbine, at approximately 1880 kPa, is heated in a regenerator against the cathode exhaust gas within the SOFC module, and then supplied to the central injection tubes of the tubular fuel cells for further preheat prior to entering the cathode side of the cells. The gas turbine also provides the small quantity of pressurized air required by the warm gas cleanup unit.

The anode exhaust gas after heat recovery is fed to a shift unit where the remaining CO is converted to CO₂ while generating

H₂. The shifted gas, now mainly CO₂ with the H₂ formed and residual CO content goes to a H₂ membrane separator to capture the H₂ [9] which is compressed and recycled to the SOFC. Alternately, a shift/membrane unit can be utilized. The non-permeate is fed to a catalytic combustor using O₂ from the ITM unit to fully remove the small amounts of any remaining CO and H₂, leaving CO₂, H₂O, and trace amount of O₂ in the stream. This stream is cooled and then pressurized (and dehydrated) to 15,200 kPa [7].

A fraction of the hot depleted air exiting the SOFC is preheated to about 800 °C, by directly combusting hot depleted air with a fraction of recycled hydrogen to maintain the temperature required by the ITM unit for air separation. The remainder of the SOFC exhaust is bypassed in order to minimize the fuel (H₂) used in preheating the feed gas to the ITM unit. In the ITM unit, O₂ is removed from the already vitiated air and exits the unit at sub-atmospheric pressure. The O₂, assumed to be essentially 100%, is cooled and compressed to gasifier pressure with a small side stream going to the catalytic “cleanup” for oxidizing combustibles remaining in the CO₂ stream. The non-permeate stream from ITM, now reduced in mass flow and slightly in pressure, is combined with the fraction of the cathode exhaust air that bypassed the ITM, and is then expanded in the gas turbine while the exhaust is fed to the heat recovery steam generator (HRSG). The gas turbine output is significantly reduced because of its low firing temperature, around 750 °C and the reduced flow.

The gasifier O₂ after compression is humidified in a counter current packed column utilizing process condensate, and is then sent to the mixing zone of the ATR gasifier. The humidification operation generates the entire steam required for the ATR while reducing the amount of wastewater to be treated. The bottoming cycle in the power block consists of the gas turbine followed by a non-reheat steam cycle. High pressure superheated steam at 10,880 kPa and 538 °C is supplied to the steam turbine while intermediate pressure (IP) steam at 2600 kPa is extracted from the steam turbine for addition to the syngas upstream of the methanator for carbon control while low pressure (LP) steam at 470 kPa is extracted for the coal drying operation. Char and purged bed material are fed to the sulfator that combusts the char while oxidizing the sulfides. Calcium sulphide being an unstable compound is oxidized to calcium sulphate which is a stable compound. The heat generated is recovered by producing high pressure steam as well as preheating the combustion air required by the sulfator [7].

3. Sensitivity analysis

The sensitivity analysis of the baseline system design is discussed under two categories (a) applying DOEx [10] using the factors and responses considered for analysis and (b) parametric analysis using APSAT on the factors to understand the cycle behavior and verify DOEx results.

3.1. Design of experiments

In parametric analysis, we analyze the system on the basis of one factor at a time. DOEx helps in identifying any higher order interaction (two or higher factor interaction (FI)) and the

Table 3
List of factors and responses

	Range
Factors	
SOFC pressure (bar)	10–20
SOFC voltage (V)	0.75–0.85
SOFC fuel utilization (%)	80–90
ATR carbon conversion (%)	90–99
Responses	
Net system efficiency (%)	To be maximized
SOFC power (MW)	To be optimized

optimum values of the significant factors specific to the response [10]. Four design parameters are considered in this study, namely the SOFC pressure, SOFC voltage, SOFC fuel utilization (SOFC Uf) and the ATR carbon conversion (ATR CC). Two responses are sought: the net system efficiency and the SOFC stack power. The SOFC stack power output (for a given coal input) is chosen as a response in addition to the net system efficiency because it is the most significant (~70% of total gross power) power producing component in the plant. Thus, in the DOEx design set, with these four factors and the two responses, there are a total of 2⁴ experiments, with repeats to estimate the error margin as shown in Table 3.

The DOEx involves the following steps for identification of the significant factors: (a) construction of a design matrix comprising the factors and responses as shown in Table 3, (b) performing an analysis of variance (ANOVA) on the design set, (c) checking for validity of the model and verifying if the model is significant and (d) plotting a half-normal plot as shown in Figs. 2 and 3. The distance of each significant factor from the line (which is drawn through the maximum possible data points as shown in Figs. 2 and 3) is directly proportional to the contribution of the factor associated with the corresponding data point for a particular response.

Fig. 2 illustrates the half-normal plot which identifies the four significant 1FI and shows lack of 2 or higher significant FI. SOFC pressure is the most significant factor followed by SOFC

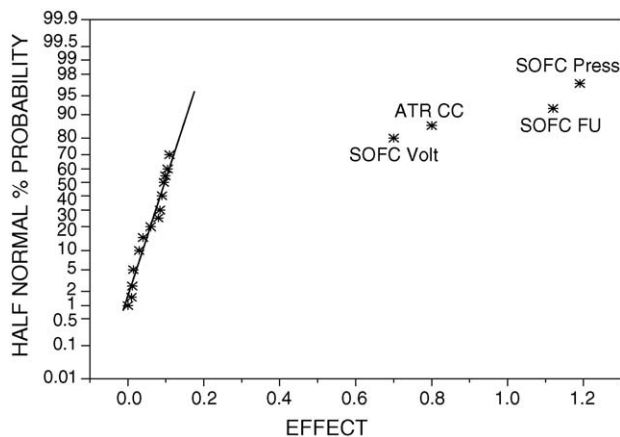


Fig. 2. Half-normal plot identifies the four significant factors (SOFC pressure, SOFC voltage, SOFC fuel utilization, and ATR carbon conversion) for the net system efficiency as response.

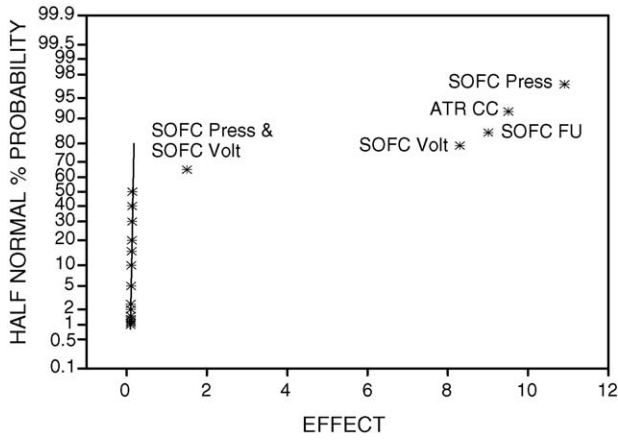


Fig. 3. Half-normal plot identifies the four significant factors (SOFC pressure, SOFC voltage, SOFC fuel utilization, and ATR carbon conversion) and one 2FI for the SOFC power output as response.

fuel utilization, ATR carbon conversion and SOFC voltage. So, for maximum system efficiency, we need to maximize the above significant factors in their respective ranges. The half-normal plot for SOFC power output on the other hand (Fig. 3) shows four 1FI (SOFC pressure, SOFC voltage, ATR carbon conversion, and SOFC fuel utilization) and a positive 2FI (SOFC pressure and SOFC voltage) as shown in Fig. 4.

The positive two-factor interaction implies that at upper limits of their respective ranges both voltage and pressure will result in a net increase in SOFC power output, which should be greater than the summation of individual increase due to each factor. In Fig. 4, the dotted line shows the positive 2FI in the form of higher slope than the reference solid line. The major outcomes of this analysis are (a) identification of the significant factors and (b) the finding that a 2FI occurs in case of SOFC power output. The next step is to investigate the system behavior using the APSAT code which includes a model for SOFC, based on first principles as well as models for the other subsystems in the plant, such as the gas and steam turbines, membranes, various reactors, humidifiers and heat exchangers. This provides verification, and thus, a scientific base for the results obtained through DOEx and insight into the cycle behavior.

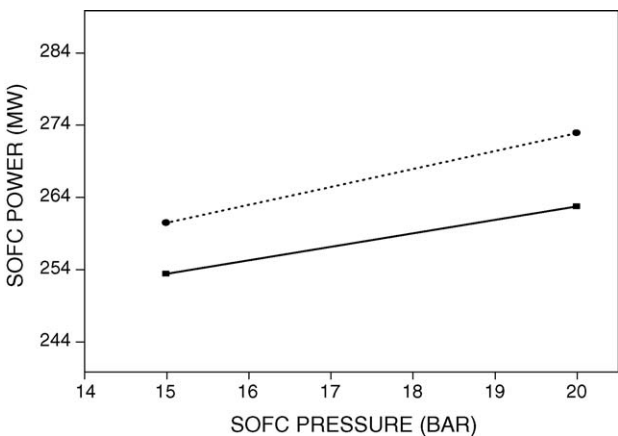


Fig. 4. Interaction plot shows the presence of 2FI in case of SOFC power output.

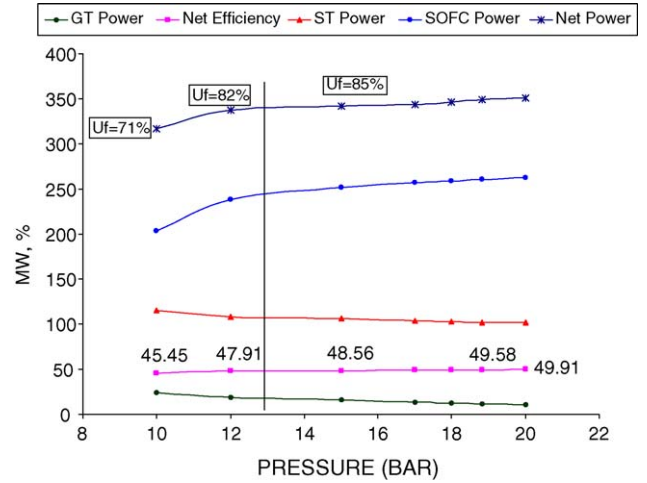


Fig. 5. Effect of pressure on system performance (Uf, fuel utilization).

3.2. Parametric analysis

The parametric analysis is performed in order to understand the responses of the critical components, such as the SOFC, ITM, gas turbine, and steam turbine to the factors which govern the behavior of the system. Each of these factors, as seen from the half-normal plots has a significant impact on the overall system thermal efficiency. The parametric analysis is performed on the baseline system using the four key factors: SOFC pressure, SOFC voltage, SOFC fuel utilization, and ATR carbon conversion.

3.2.1. SOFC pressure

As seen from Fig. 5, the net system efficiency increases as the pressure increases. As the pressure is increased, the net power developed by the gas turbine is decreased (increase in the power required by the gas turbine compressor as the operating pressure is raised is much higher than that produced by the gas turbine expander). A similar trend is seen in case of steam turbine power output, which shows a decreasing trend as the pressure is increased. This is due to decrease in temperature of gas turbine exhaust entering the heat recovery steam generator.

Fig. 6 shows the effect of changing the inlet pressure of the SOFC (by increasing the pressure ratio of the power recovery expander located upstream of the SOFC) on the depleted air flow exiting the ITM, the amount of cathode exhaust gas by-passed around the ITM as well as the overall fuel utilization, i.e., based on electrochemically oxidizing the fresh (make-up) syngas + the H₂ recovered downstream of the fuel cell by the membrane unit and recycled back to the fuel cell.

As the operating pressure of the SOFC is decreased, the partial pressure of the O₂ in the ITM feed gas also decreases. As a result, the driving force for separating the O₂ is decreased. For a given amount of O₂ production as demanded by the gasifier and the catalytic combustor (to oxidize the residual amounts of combustibles present in the raw CO₂ stream) and a given amount of feed gas to the ITM, the recovered O₂ product pressure tends to decrease as the ITM feed gas pressure decreases. The O₂ recovery pressure, however, was held constant (at the same reasonable

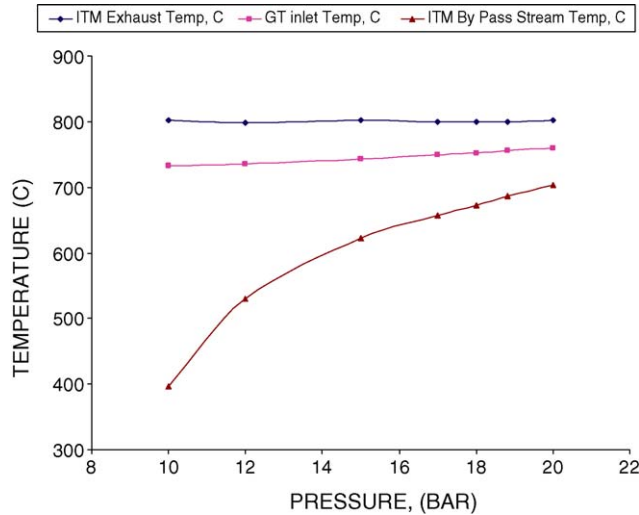


Fig. 6. Effect of pressure on gas turbine inlet temperature.

value as in the base case in order to limit the size of the ITM unit) by by-passing a lesser fraction of the depleted air (cathode exhaust after heat exchange) around the ITM, i.e., increasing the amount of feed gas to the ITM. As more feed gas is supplied to the ITM, the demand for the fuel (H_2) to preheat the feed gas to the required operating temperature of the ITM ($800^\circ C$) is also increased (Fig. 7) (the H_2 is recovered from the depleted fuel, i.e., anode exhaust gas after heat exchange, by the membrane unit downstream of the SOFC). This leaves less H_2 for recycle to the SOFC which in turn reduces the power output of the SOFC.

As the SOFC operating pressure is further reduced (below about 13 bar), a point is reached where the total amount of H_2 recovered is less than that required to preheat the ITM feed gas. The per-pass fuel utilization (U_f) has to be decreased in order to have enough H_2 for recovery and use for preheating the ITM feed gas (Fig. 8). The SOFC power output and the overall system efficiency, are thus, significantly affected in this region of operating pressure (SOFC system inlet pressure <13 bar). The overall fuel utilization decreases with a decrease in the SOFC pressure over

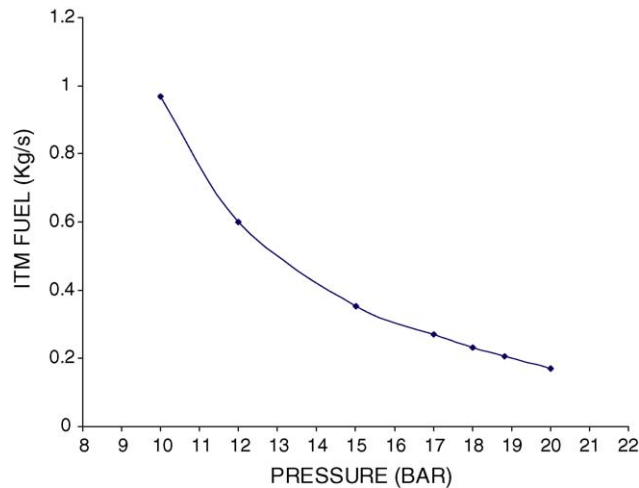


Fig. 7. Effect of pressure on feed flow rate going into the ITM.

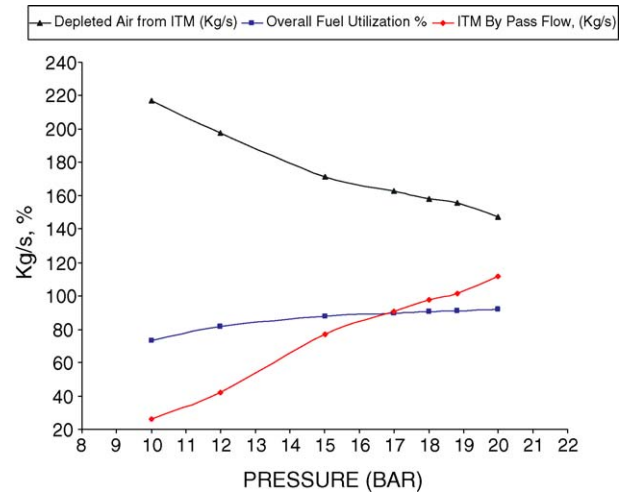


Fig. 8. Effect of SOFC pressure on critical parameters.

this entire region of operating pressures (i.e., <13 bar) due to the increase in the H_2 required for pre-heating the ITM feed downstream of SOFC. The H_2 required for the combustor upstream of the ITM unit decreases as we increase the system pressure, which increases the amount of H_2 available for recycles to the SOFC. As the pressure increases, the pressure ratio across the turbine goes up, and therefore, more work is extracted through the gas turbine expander at higher pressure. As mentioned earlier, this leads to a decrease in inlet temperature to the HRSG thereby lowering the steam turbine power output.

3.2.2. SOFC fuel utilization

The effect of varying the SOFC fuel utilization on system performance is presented in Fig. 9. As expected, the SOFC power output and the overall system efficiency increase as the fuel utilization is increased. As the fuel utilization increases, the gas turbine power output increases due to increase in SOFC cathode exhaust temperature (the heat generated within the fuel cell also increases as more fuel is reacted inside the SOFC leading to a higher cathode exhaust temperature). On the other hand, as the fuel utilization goes up, the mass flow rate of the cathode exhaust

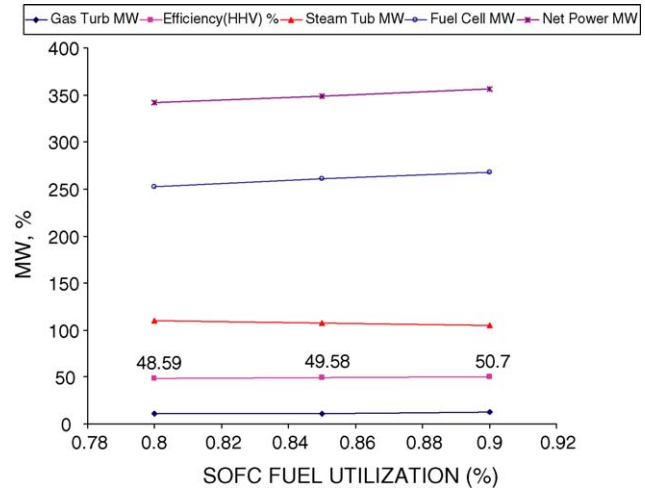


Fig. 9. Effect of SOFC fuel utilization on system performance.

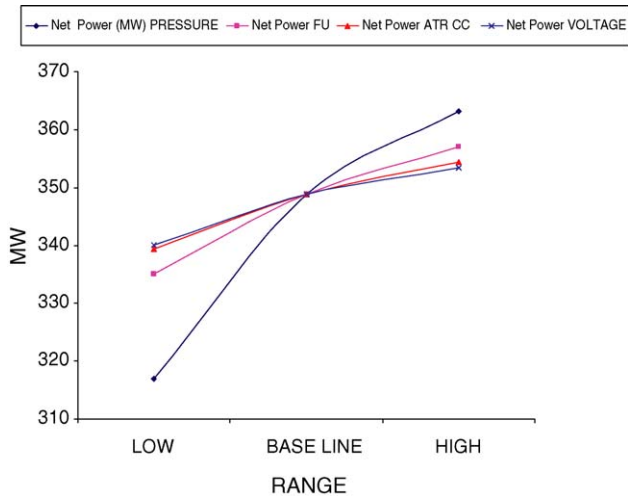


Fig. 10. Individual effect of each significant factor on net power output.

gas decreases since more O_2 is transported from the cathode to the anode side. Thus, the amount of gas entering or leaving the gas turbine or entering the HRSG decreases. This results in lowering the steam production in the HRSG, and consequently a decrease in the steam turbine power output (the effect of reduced flow rate far outweighs the increase in the temperature). As a result, the increase in net power output in the case of increased SOFC fuel utilization is less than the increase in the net power output in case of increased SOFC pressure (Fig. 10).

3.2.3. ATR carbon conversion

Fig. 11 shows quantitatively the improvement in the overall system performance as the carbon conversion within the gasifier is varied. As the carbon conversion is decreased, a greater fraction of the coal bound energy is available as chemically bound energy in the syngas for conversion in the SOFC such that the overall system performance is improved. On the other hand, the steam generated in the sulfator where the unconverted carbon is combusted is increased as the gasifier carbon conversion is reduced and the accompanying increase in steam turbine power output compensates somewhat the decrease in the power output of the SOFC and the gas turbine, making the effect of carbon

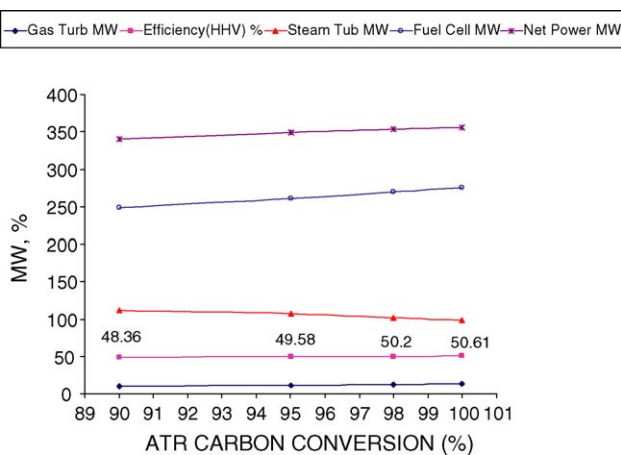


Fig. 11. Effect of ATR carbon conversion on system performance.

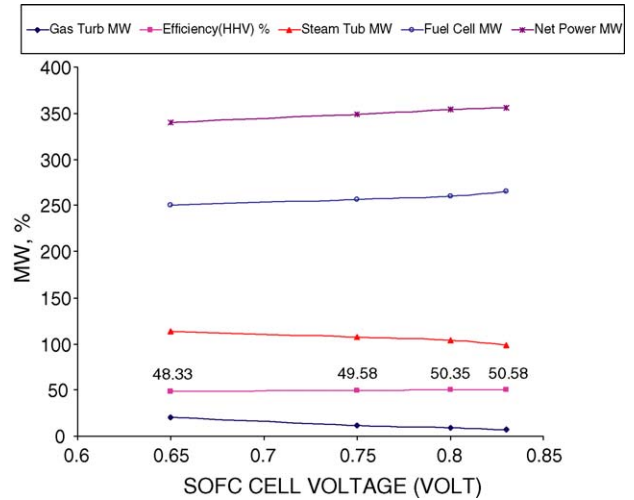


Fig. 12. Effect of SOFC voltage on system performance.

conversion on system performance less significant than the effect of SOFC pressure and its fuel utilization (Fig. 10).

3.2.4. SOFC cell voltage

The effect of varying the SOFC cell voltage on system performance is presented in Fig. 12. As expected, the SOFC power output increases as the cell voltage is increased. As the cell voltage is increased, the gas turbine power output decreases due to lower gas turbine inlet temperature. As a result, the gas turbine exhaust temperature also decreases which causes a decrease in the steam production in the HRSG resulting in lower steam turbine power output. The decrease in the power output of the gas and the steam turbines, however, is far outweighed by the increase in the SOFC power output when the cell voltage is increased, and consequently, the overall net power output and system thermal efficiency are increased.

4. Results

The results obtained by the DOEx and APSAT (the parametric analysis) are further analyzed in order to provide insight towards system modifications in order to improve the plant performance. The performance of the new system, thus, developed is then generated utilizing APSAT.

4.1. DOEx and APSAT

The combined analysis of DOEx and APSAT on the baseline system design confirms that pressure is the most significant factor for overall system efficiency. As pressure increases (a) the SOFC power output increases (which forms as much as 70% of the gross power output), (b) the steam turbine power output decreases (which forms about 25% of the gross power output) but the decline is relatively small in the high pressure range of 15–20 bar, and (c) the gas turbine power output decreases, but the effect of the decrease in gas turbine power output is quite small on the total plant output (contributes 5% of the gross power output).

As explained earlier, in case of SOFC fuel utilization, SOFC power output also increases while the steam turbine power out-

put decreases, and the gas turbine power output increases as the fuel utilization increases. The positive impact of gas turbine power output on the other hand is offset by the steam turbine power output due to higher contribution of steam turbine (25% of gross power output). Thus, as seen from Fig. 3, the overall improvement in system performance is more significant with respect to the SOFC pressure than the fuel utilization. As a result a lower net power output is achieved in comparison to SOFC pressure (Fig. 10) because of (a) lower SOFC power output and (b) lower combined output of steam turbine and gas turbine.

The effect of ATR carbon conversion on system performance is even lower as compared to the SOFC operating pressure and its fuel utilization as seen from the relative slopes of the lines shown in (Fig. 10). This is due to, a steep decline in steam turbine power output as the carbon conversion is increased as shown by the parametric analysis using APSAT. Furthermore, the ATR carbon conversion has a lower impact than the SOFC pressure and fuel utilization on power output of the SOFC (Fig. 3) making the effect of the ATR carbon conversion less significant on the overall system thermal performance.

Finally, as shown in Fig. 12, as the voltage is increased, both the gas turbine and the steam turbine power outputs decrease, while the SOFC power output increases. The increase in SOFC power output is least due to change in voltage as compared to the other three factors (SOFC pressure, SOFC voltage, and ATR CC) (Fig. 3). As a result the SOFC voltage is the least significant among the four significant factors in the ranges considered.

In case of SOFC power output (Fig. 3), DOEx points out a 2FI of SOFC pressure and its voltage (Fig. 4). Under constant fuel utilization, as the pressure increases, the recycle flow of hydrogen to SOFC increases because the demand for fuel in the combustor downstream of SOFC decreases. Next, as the SOFC voltage is increased, the per cell efficiency increases, while the per cell current density decreases. To maintain the same system current, the number of cells in the SOFC stacks increases.

Thus, due to the combined increase in (a) SOFC voltage which is equivalent to increasing the per cell efficiency and the higher number of cells in the SOFC stack and (b) SOFC pressure which results in an increase in the amount of fuel entering the SOFC anode, the power output of the SOFC stack increases more than the individual increases due to the SOFC pressure and voltage.

4.2. System design modification

The DOEx and APSAT combined analysis shows that among the four significant factors, it is the SOFC pressure and its fuel utilization that are the more important factors for further investigation. The net system efficiency of the baseline system is 49.58% on HHV basis. Further increases in the system thermal efficiency may be realized by increasing the SOFC pressure but development of such SOFC poses several technical challenges. System modifications will be sought to increase the SOFC fuel utilization (on an overall plant basis), the second most significant factor. It will be highly desirable for the new system to have the added advantage of less dependency of the thermal performance on the SOFC pressure. Note that in the baseline system

design, as the SOFC pressure is decreased, the amount of fuel required in the combustor downstream of SOFC increased and to meet the demand for extra fuel in the combustor, the SOFC fuel utilization had to be reduced.

To address this issue the following modifications are made to the baseline design (a) elimination of the combustor downstream of SOFC and upstream of ITM in order to maximize the H₂ recycled to the SOFC, and thus, increase the overall fuel utilization and (b) add a heat exchanger upstream of the SOFC to preheat the air entering the SOFC cathode such that the SOFC exhaust temperature is 800 °C as required by the ITM. Fig. 13 represents the resulting new design.

4.3. System design comparison

Fig. 14 shows the positive impact of these design modifications which result in (a) a higher overall system efficiency for a given SOFC operating pressure and (b) a lower sensitivity of the SOFC operating pressure on the overall system efficiency as compared to the baseline system design especially in the lower pressure regime from 10 to 15 bars. The new design has a significant advantage from industry stand point as it provides significant lower penalty as compared to baseline system design on overall system efficiency at lower pressures (10 and 12 bar). Fig. 15 shows the comparison between the major power producing components in the baseline system design and the new system design. In the new system design as the pressure is increased, the SOFC power output decreases, but remains higher than the baseline design in the entire pressure range. This is due to slight decrease in the recycle amount of hydrogen entering the SOFC as pressure increases, conversion of the small amount of CH₄ present in the feed gas to the reformer being limited as the pressure increases. As the pressure is increased, the recycle flow decreases but the total fuel entering the SOFC is much higher than the baseline case due to lack of fuel demand in the ITM unit downstream of SOFC. In the baseline system design, however, the SOFC power output increases as pressure increases due to reduced fuel demand by the ITM combustor, the ITM feed gas flow rate being lower.

In the new system design, the gas turbine power output increases as pressure increases due to higher turbine inlet temperature and mass flow rate which more than compensate for the increase in compression power (Fig. 16). In case of the baseline system design, however, a decrease in the gas turbine power output with increase in pressure is seen due to higher compression power which more than offsets the increase in the turbine power due to the higher turbine inlet temperature, the increase in this temperature being less significant as compared to the new system design. The increase in the turbine inlet temperature in the new system design is more significant because the entire amount of H₂ captured downstream of the SOFC for recycle (which decreases with an increase in pressure as seen in Fig. 17) is available for the SOFC while the unconverted energy is available for the bottoming gas turbine.

In the new system design, as the SOFC pressure is increased, the steam turbine power output increases due to increase in the steam generation caused by an increase in the temperature of

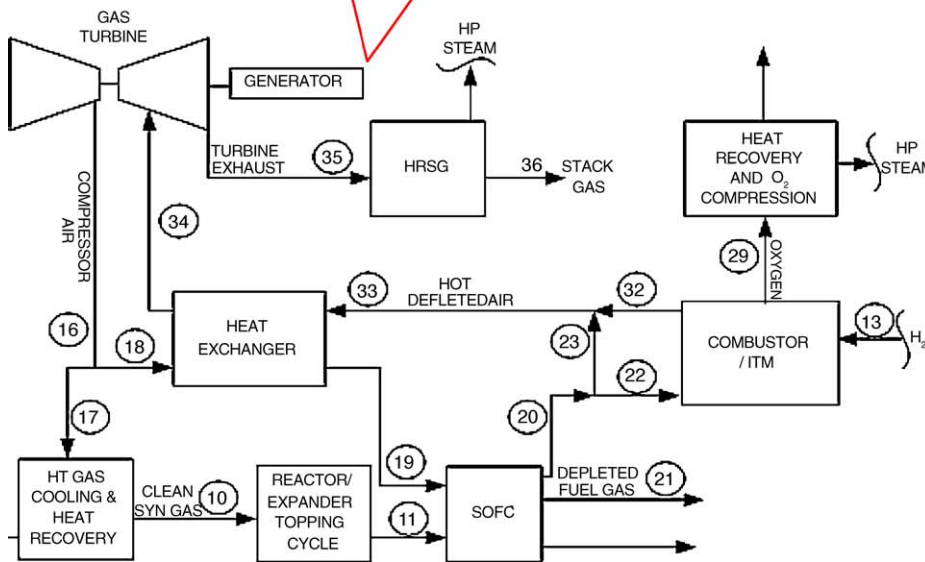
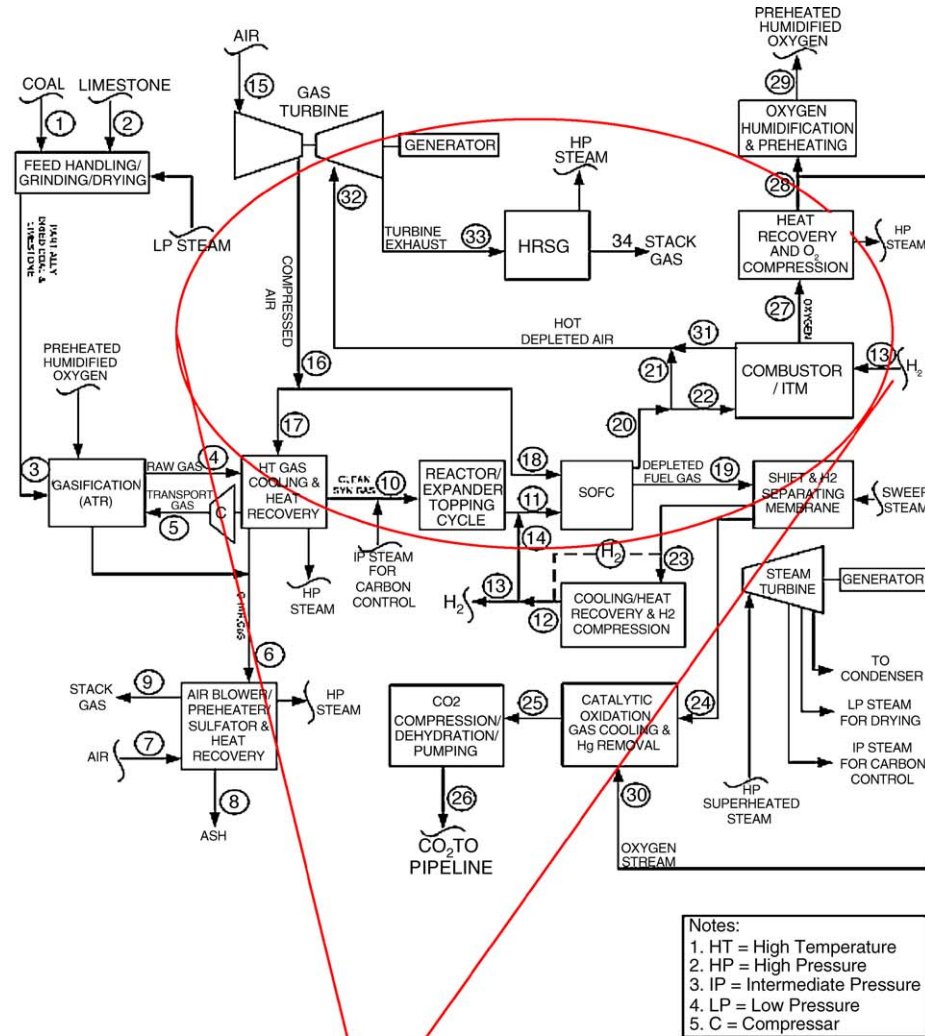


Fig. 13. Block flow sketch showing a section of baseline plant design replaced by new design.

the gas turbine exhaust entering the HRSG. In baseline system design on the other hand, the steam turbine power output decreases with increase in pressure since the gas turbine exhaust temperature decreases.

Although the trend remains the same in the entire pressure range, a much larger gap between the net system power output is seen (Fig. 15) in the low pressure region (10–15 bar) as compared to high pressure region (15–20 bar) due to the follow-

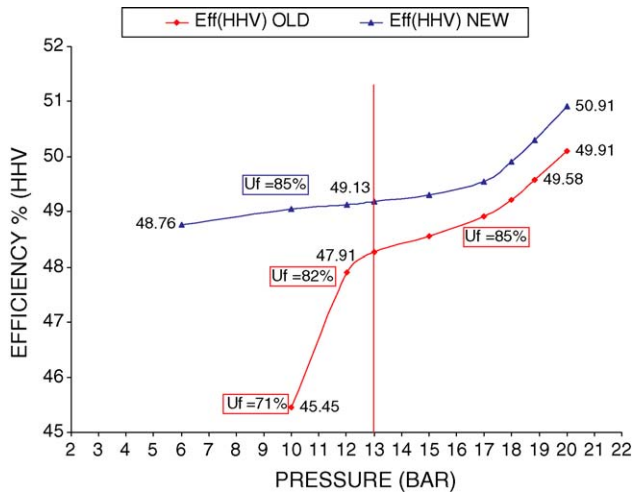


Fig. 14. Effect of pressure on system efficiency for new and baseline system design.

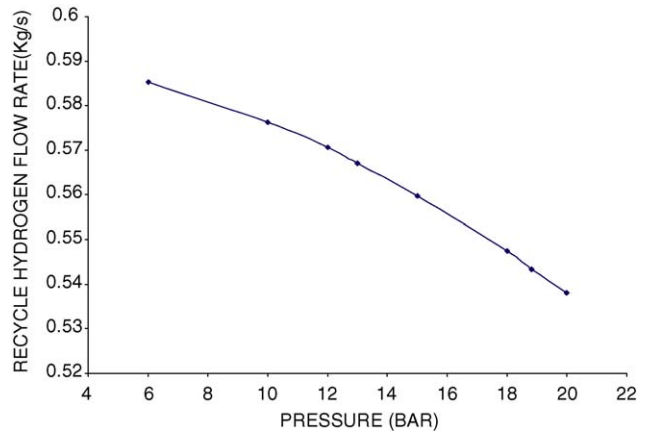


Fig. 17. Effect of pressure on hydrogen recycle flow rate in case of new system design.

Table 4

Comparison table between baseline and new system design for baseline performance

Parameter	Baseline system	New system
SOFC output (MW)	273.368	260.73
GT output (MW)	11.51	1.41
ST output (MW)	101.02	104.5
Net power (MW)	348.01	353.01
Net efficiency (HHV) (%)	49.58	50.3

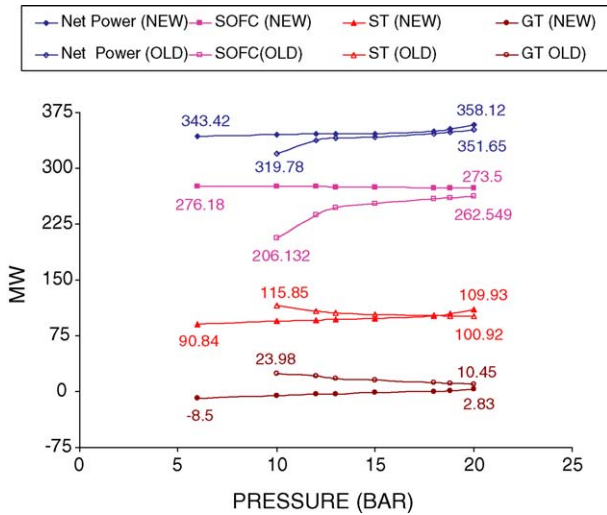


Fig. 15. Comparison plot of new and baseline system design performance as a function of pressure.

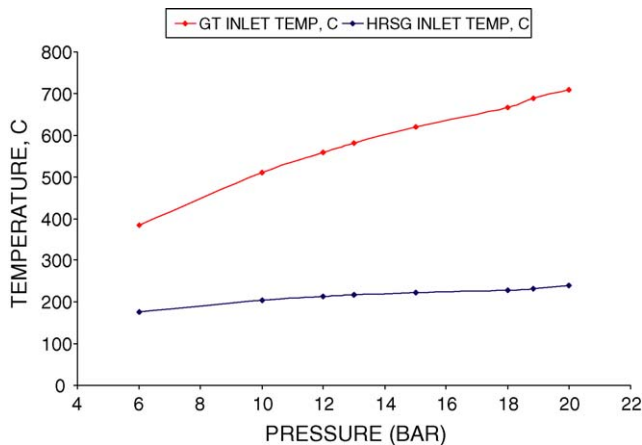


Fig. 16. Effect of pressure on new system design critical parameters.

ing reasons: first, in the low pressure zone, the baseline system design has limitation on SOFC fuel utilization. As a result, at lower pressure, the SOFC system is operated at lower fuel utilization due to higher fuel demand inside the combustor, which is not the case in new system design in which, the consumption of fuel inside the SOFC is higher, due to elimination of the combustor downstream of SOFC. Second, lowering pressure has a positive influence on the SOFC power output in case of the new system design as compared to negative influence in the baseline system design. The major system performance parameters for the two designs are compared in Table 4.

The new system design with a system efficiency of 50.3% on HHV basis is slightly more efficient than the baseline design at baseline pressure of 18.8 bar but in the low pressure region, the new system efficiency shows a significant increase in efficiency over the baseline design, as much as 7.3% decrease in the heat rate at a pressure of 10 bar, this pressure being in the region of interest to the developers of pressurized SOFCs.

5. Conclusion

The key points summarizing the paper are:

- (a) Identification of significant factors affecting the system performance. The most significant being the SOFC pressure, followed by SOFC fuel utilization, ATR carbon conversion, SOFC voltage, and the response being the net system efficiency.
- (b) In case of SOFC power output as response, along with the four significant single factors namely the SOFC pressure,

SOFC fuel utilization, ATR carbon conversion, and SOFC voltage, there is a positive 2FI of SOFC pressure and SOFC voltage.

- (c) System design modifications (eliminating the combustor downstream of SOFC and adding a heat exchanger upstream of SOFC to preheat the inlet cathode stream) lead to an increase in net system efficiency.
- (d) The impact of pressure on system efficiency is reduced with the new system design. The impact is most significant in the lower pressure region where a relative increment of 7.3% in efficiency is realized at 10 bar.
- (e) The maximum system efficiency under the given constraints of cost is 53.64% (includes the CO₂ sequestration) on HHV basis using coal. The penalty for CO₂ sequestration is less than 0.5% on net system efficiency on HHV basis due to the efficient system design.

Acknowledgements

The U.S. Department of Energy provided financial support for this research under contract number DE-FC26-00HT40845.

References

- [1] A.D. Rao, A.Verma, G.S. Samuelsen, Engineering and economic analysis of a coal based solid oxide fuel cell hybrid power plant, Proceedings of GT2005: ASME Turbo Expo, Power for Land, Sea and Air, 2005.
- [2] DOE, Vision 21 Program Plan—Clean Energy Plants for the 21st Century US Department of Energy, 1999.
- [3] A.D. Rao, A Thermodynamic Analysis of Tubular SOFC Based Hybrid Systems, Engineering, University of California, Irvine, 2000.
- [4] A.D. Rao, G.S. Samuelsen, Analysis strategies for tubular solid oxide fuel cell based hybrid systems, J. Eng. Gas Turb. Power 124 (2002) 503–509.
- [5] P.A. Armstrong, Method for Predicting Performance of an Ion Transport Membrane Unit-Operation, Advanced Gas Separation Technology, Air Products and Chemicals, Inc., Allentown, PA.
- [6] R.E. Richards, P.A. Armstrong, M.F. Carolan, V.E. Stein, R.A. Cutler, J.H. Gordon, D.M. Taylor, Developments in ITM oxygen technology for integration with advanced power generation systems, in: Proceedings of the 26th International Technical Conference on Coal Utilization and Fuel Processing, March, 2001.
- [7] G.S. Samuelsen, A.D. Rao, FutureGen and Advanced Power Plant Development and Analyses Methodologies, Second Semi-annual Report 2004, Award No. DE-FC26-00NT40845, January 31, 2005.
- [8] A.D. Rao, Reactor Expander Topping Cycle, U.S. Patent No. 4,999,993 (March 19, 1991).
- [9] R.E. Roark, R. Machay, A.F. Sammells, Hydrogen separation membranes for Vision 21 energy plants, in: Proceedings of the 28th International Technical Conference on Coal Utilization and Fuel Systems, Clearwater, FL, March 10–14, 2003.
- [10] R.L. Mason, R.F. Gunst, J.L. Hess, Statistical Design and Analysis of Experiments with applications to Engineering and Science, second ed., Wiley Series in Probability and Statistics, 2003.